SUPPLEMENTARY DATA

Towards Optimization of Imaging System and Lymphatic Tracer for Near-Infrared Fluorescent Sentinel Lymph Node Mapping in Breast Cancer

J. Sven D. Mieog, M.D.[1,*], Susan L. Troyan, M.D. [2,*], Merlijn Hutteman, M.Sc.[1,3,*], Kevin J. Donohoe, M.D.[4], Joost R. van der Vorst, M.D.[1], Alan Stockdale, M.Ed.[3], Gerrit-Jan Liefers, M.D., Ph.D.[1], Hak Soo Choi, Ph.D.[3], Summer L. Gibbs-Strauss, Ph.D.[3], Hein Putter, Ph.D.[5], Sylvain Gioux, Ph.D.[3], Peter J.K. Kuppen, Ph.D.[1], Yoshitomo Ashitate, M.D.[3], Clemens W.G.M. Löwik, Ph.D.[6], Vincent T.H.B.M. Smit, M.D., Ph.D.[7], Rafiou Oketokoun, M.S.[3], Long H. Ngo, Ph.D.[8], Cornelis J.H. van de Velde, M.D., Ph.D.[1], John V. Frangioni, M.D., Ph.D.[3,4,†] , and Alexander L. Vahrmeijer, M.D., Ph.D.[1,†]

[1] Departments of Surgery, [5] Medical Statistics, [6] Endocrinology, and [7] Pathology,
Leiden University Medical Center, Leiden, the Netherlands
[2] Breast Care Center, Department of Surgery, [3] Division of Hematology/Oncology, Department of Medicine, [4] Department of Radiology, and [8] Division of General Medicine, Department of Medicine,
Beth Israel Deaconess Medical Center, Boston, MA 02215

* These authors contributed equally to the study and share first authorship.

† **Corresponding Authors:** John V. Frangioni, M.D., Ph.D.
Beth Israel Deaconess Medical Center
330 Brookline Avenue, Room SL-B05, Boston, MA 02215
Phone: 617-667-0692 Fax: 617-667-0981
Email: jfrangio@bidmc.harvard.edu

Dr. Alexander L. Vahrmeijer, M.D., Ph.D.
Albinusdreef 2, 2300 RC Leiden, The Netherlands
Phone: +31715262309 Fax: +31715266750
Email: a.l.vahrmeijer@lumc.nl

SUPPLEMENTARY METHODS

Preparation of the NIR Fluorescent Lymphatic Tracer for Large Animal Studies and the 6-Patient Pilot Clinical Study: Indocyanine green (ICG) USP (25-mg vials) was purchased from Akorn (Decatur, IL) and resuspended in 10 cc of supplied diluent to yield a 2.5-mg/ml (3.2 mM) stock solution. Various amounts of this stock solution were transferred to a 50-cc bag of Buminate (25% human serum albumin [HSA] solution; Baxter Healthcare, Deerfield, IL) to yield ICG in HSA (ICG:HSA) at a final concentration of 10 μM, 125 μM, 250 μM, or 500 μM.

Mini-FLARE™ Imaging System Hardware: The portable cart and imaging system pole were from Yankee Modern Engineering (Groton, MA). The gooseneck arm (#810-205) was from Civco (Kalona, IA). Monitor brackets were from GCX (Petaluma, CA). The isolation transformer (#ISB-100M) was from Toroid (Salisbury, MD) and the power supply (#AC3-00NM-00-H) was from Cosel (San Jose, CA). The model T5400 computer, ultra-sharp DVI monitors (20”), and monitor splitter were from Dell (Round Rock, TX). The multifunction DAQ board (#USB-6229) was from National Instruments (Austin, TX).

Computer-aided design was performed at Design and Assembly Concepts (Leander, TX). Manufacturing and black matte anodization was performed at LAE Technologies (Barrie, Ontario, Canada). Cooling of the housing was performed using a Solid State Cooling (Pleasant Valley, NY) 160 W Oasis recirculator filled with 25% USP propylene glycol in USP water and set to 15˚C. Watertight channels were engineered into the light housing. Custom optics were from Qioptiq (Fairport, NY). Light-emitting diode (LED) modules and their filtration have been described in detail previously.[1] A custom printed circuit board (PCB) within the imaging head controlled the focusing motor and LED modules. The PCB was assembled at Sure Design (Farmingdale, NJ). Optics filters, including the dichroic mirror (#HMS3060-DiInv660), dual-bandpass emission filter (#HMS3060-Em707+824) and color-video clean-up filter (#HMS3060-Em650SP) were from Chroma Technology (Brattleboro, VT).

The color and NIR Firewire (IEEE-1394) cameras were an Imitech (Seoul, Korea) model IMC-80F and a Prosilica (Burnaby, British Columbia, Canada) model EC1020, respectively. Footswitch control of the system[2] and acquisition gating[3] have been described in detail previously. Additional details can be found at www.frangionilab.org.

Mini-FLARE™ Imaging System Software: Custom software for the Mini-FLARE™ system was modified from FLARE™ imaging system software[4] to include rotation of all images in 90˚ increments

and automated cycling between 700 nm and 800 nm fluorescence excitation. The software also permitted each grayscale NIR fluorescence image (700 nm or 800 nm) to be "pseudo-colored" from a palette of over 256 visible colors and overlaid in real-time onto the color video image.

***In Vitro* Characterization:** Methylene blue (MB; 1%; 10 mg/ml) was purchased from Taylor Pharmaceuticals (Buffalo Grove, IL). ICG and MB were diluted at the indicated concentrations in phosphate buffered saline (PBS), pH 7.4 and transferred to 96-well acrylic plates. The plate was visualized using 2.3 mW/cm^2 of 670-nm excitation light or 16.8 mW/cm^2 of 760-nm excitation light, at a working distance of 8".

First-in-Human Pilot Clinical Trial of Mini-FLARE™ and Various ICG:HSA Injection Concentrations: The clinical trial was approved by the Institutional Review Board (IRB) of the Beth Israel Deaconess Medical Center and was performed in accordance with the ethical standards of the Helsinki Declaration of 1975. The IRB deemed the Mini-FLARE™ imaging system a "non-significant risk" device. All patients gave informed consent and were anonymized. Clinical trial participants were women undergoing SLN mapping for breast cancer. All subjects received standard-of-care sentinel node scintigraphic mapping performed by a single nuclear medicine physician (Dr. Donohoe) approximately 2 h prior to surgery. A total of 0.8 mCi filtered (0.22 μm Millipore filter) ^{99m}Tc-sulfur colloid buffered with bicarbonate to a pH of 7.0 was administered as 4 deep peri-tumoral injections (100 μCi in 0.3 ml each) and 4 intradermal injections (100 μCi in 0.1 ml each). In the operating room, the same nuclear medicine physician injected a total of 1.6 ml of ICG:HSA, given as 4 deep 0.3 ml peri-tumoral injections and 4 intradermal 0.1 ml injections in the same locations as the ^{99m}Tc-sulfur colloid injections. The injection sites were massaged for approximately 5 min in the operating room. Lymphatic mapping using a handheld gamma probe was performed as per standard practice except that 26,600 lux of white (400-650 nm) light illuminating the surgical field was provided by the mini-FLARE™ imaging system, which was positioned approximately 13" away from the patient. Only one (800 nm) of two available NIR fluorescence channels was utilized for this study. Excitation fluence rate for 800 nm excitation light was 7.7 mW/cm^2. Camera exposure was between 10 to 1000 msec as indicated. An SLN exhibiting a 10-sec ^{99m}Tc count rate greater than axillary background and at least 10% of the hottest sentinel node was considered positive by lymphoscintigraphy. An SLN exhibiting a signal-to-background ratio (SBR) ≥ 1.1 *in situ* was considered positive by NIR fluorescence.

SUPPLEMENTARY RESULTS

Imaging Head of the Mini-FLARE™ Imaging System and *In Vitro* Characterization: The imaging head (Supplementary Figure 1A) is a small, self-contained, water-cooled device that illuminates the surgical field using high-powered, filtered LEDs (Supplementary Figure 1B).

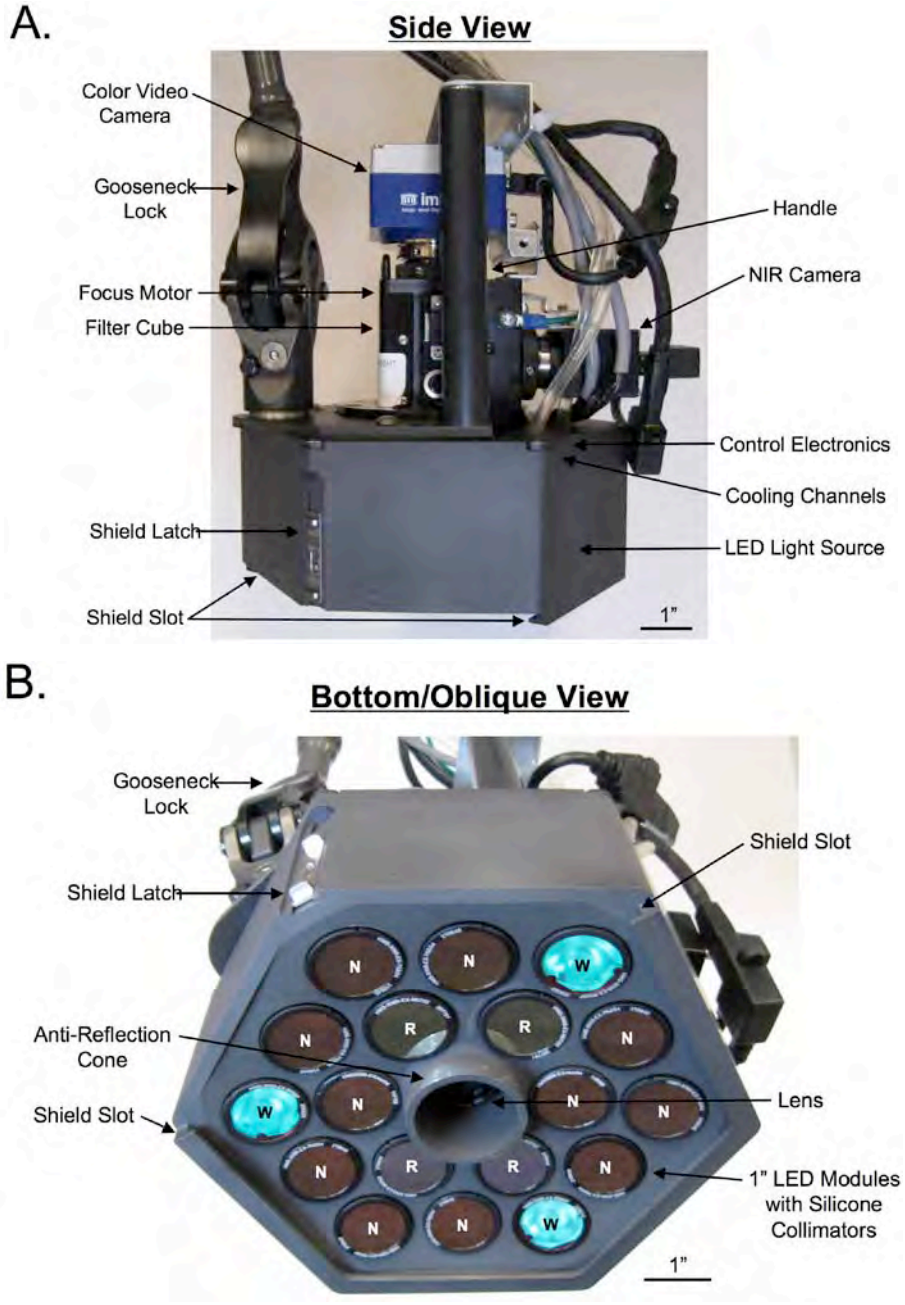

Supplementary Figure 1 – Imaging Head of the Mini-FLARE™ Portable Near-Infrared Fluorescence Imaging System: A. Side view with all major parts identified. C. Bottom/oblique view with all major parts identified. W = white light (400 to 650 nm) LED module. R = 670 nm (656-678 nm) fluorescence excitation LED module. N = 760 nm (745-779 nm) fluorescence excitation LED module.

Imaging Optics and *In Vitro* Characterization: Exact filtration bands are shown in Supplementary Figure 2. Of note, Mini-FLARE™ achieves miniaturization by using only a single grayscale camera and a dual bandpass emission filter for both NIR fluorescence emission channels, yet can still separate each channel by cycling 700 nm and 800 nm fluorescence excitation light sources on and off in sequence. As shown in Supplementary Figure 3 for the clinically available NIR fluorophores MB (700 nm) and ICG (800 nm), Mini-FLARE™ is able to separate 700 nm and 800 nm fluorescence provided that fluorophore concentrations and excitation fluence rates are adjusted appropriately.

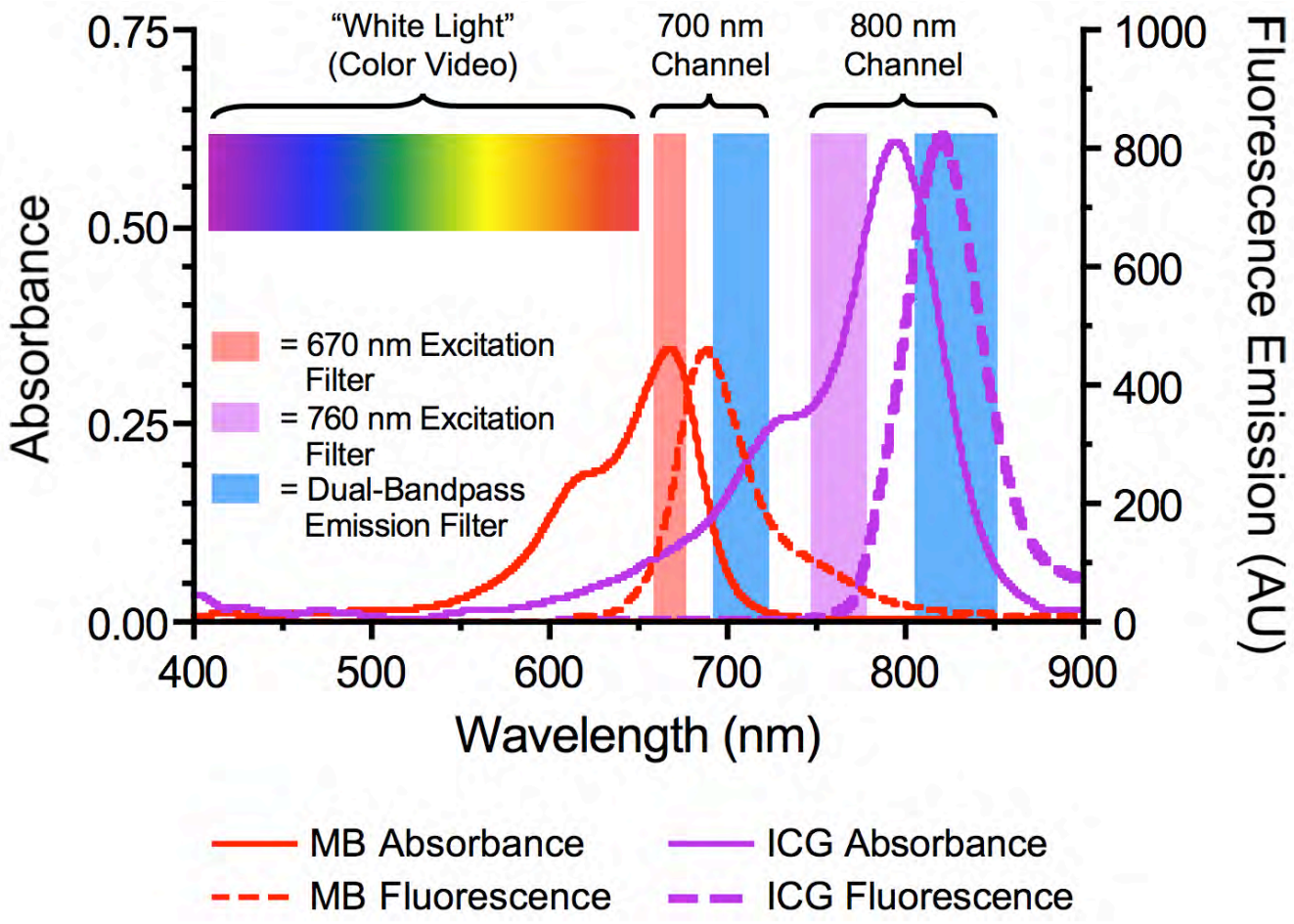

Supplementary Figure 2 – Optical Channels of the Mini-FLARE™ Imaging System: The "white light" color video channel spans 400 to 650 nm. Shown in pink and purple are the excitation light filter transmission bands for the 700 nm and 800 nm channels, respectively. The common (700 nm/800 nm) fluorescence emission channel (dual bandpass) is shown in blue. Superimposed on these optical channels are the absorbance (left axis, solid curves) and fluorescence spectra (right axis, dashed curves) for 5-µM methylene blue (MB; red) and 5-µM indocyanine green (ICG; purple) in 100% serum, pH 7,4.

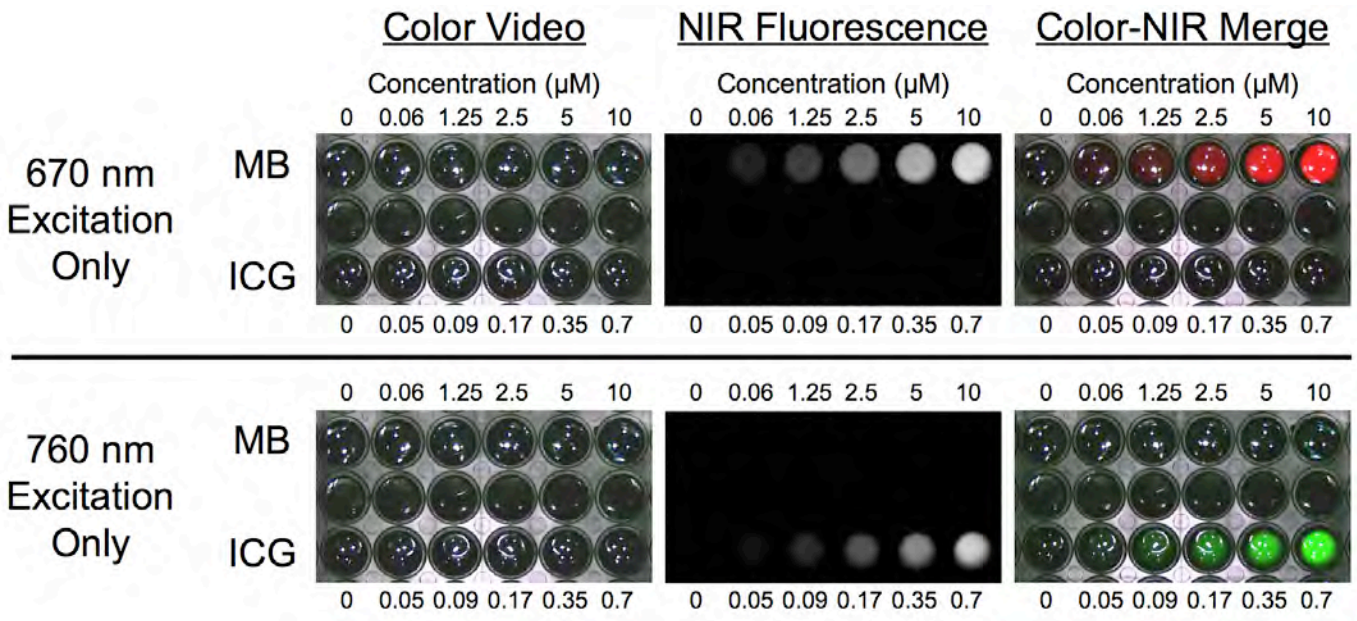

Supplementary Figure 3 – Optical Isolation of 700-nm and 800-nm Channels: Shown are increasing concentrations of methylene blue (MB; top rows of plate) in phosphate-buffered saline, pH 7.4 and indocyanine green (ICG; bottom rows of plate) in dimethylsulfoxide (DMSO), all in wells of a 96-well plate. Shown are Mini-FLARE™ images from color video (left), NIR fluorescence (middle), and a pseudo-colored (red = MB, green = ICG) merge of the two. Camera exposure time was 60 msec. The slightly smaller diameter of ICG is due to a lack of meniscus formation in DMSO.

First-in-Human Clinical Trial in Breast Cancer SLN Mapping: The primary objective of the 6-patient first-in-human clinical trial was to determine whether Mini-FLARE™ was safe and did not interfere with the standard of care. A secondary endpoint was to begin to explore the complex relationship between NIR fluorophore injection concentration and final SBR in the SLN. Study subject characteristics are provided in Supplementary Table 1. Of note, there was significant variability in body habitus, primary tumor size, and histological type among the study subjects.

There were no adverse events associated with the Mini-FLARE™ imaging system and no ergonomic issues that altered the standard of care. Shown in Supplementary Table 2 are the radioactive count rates for each SLN identified using ^{99m}Tc-sulfur colloid and the corresponding NIR fluorescence signal measured using Mini-FLARE™ during SLN mapping of breast cancer. Shown in Supplementary Figure 4 are typical real-time intraoperative imaging results. Of note, the SBR of the *in situ* SLN is highly dependent on the location of the sinus entry point relative to the surgical incision. It is often necessary to rotate the SLN until the sinus entry point is "facing up" to achieve the highest possible SBR, although some fluorescence is seen from all angles.

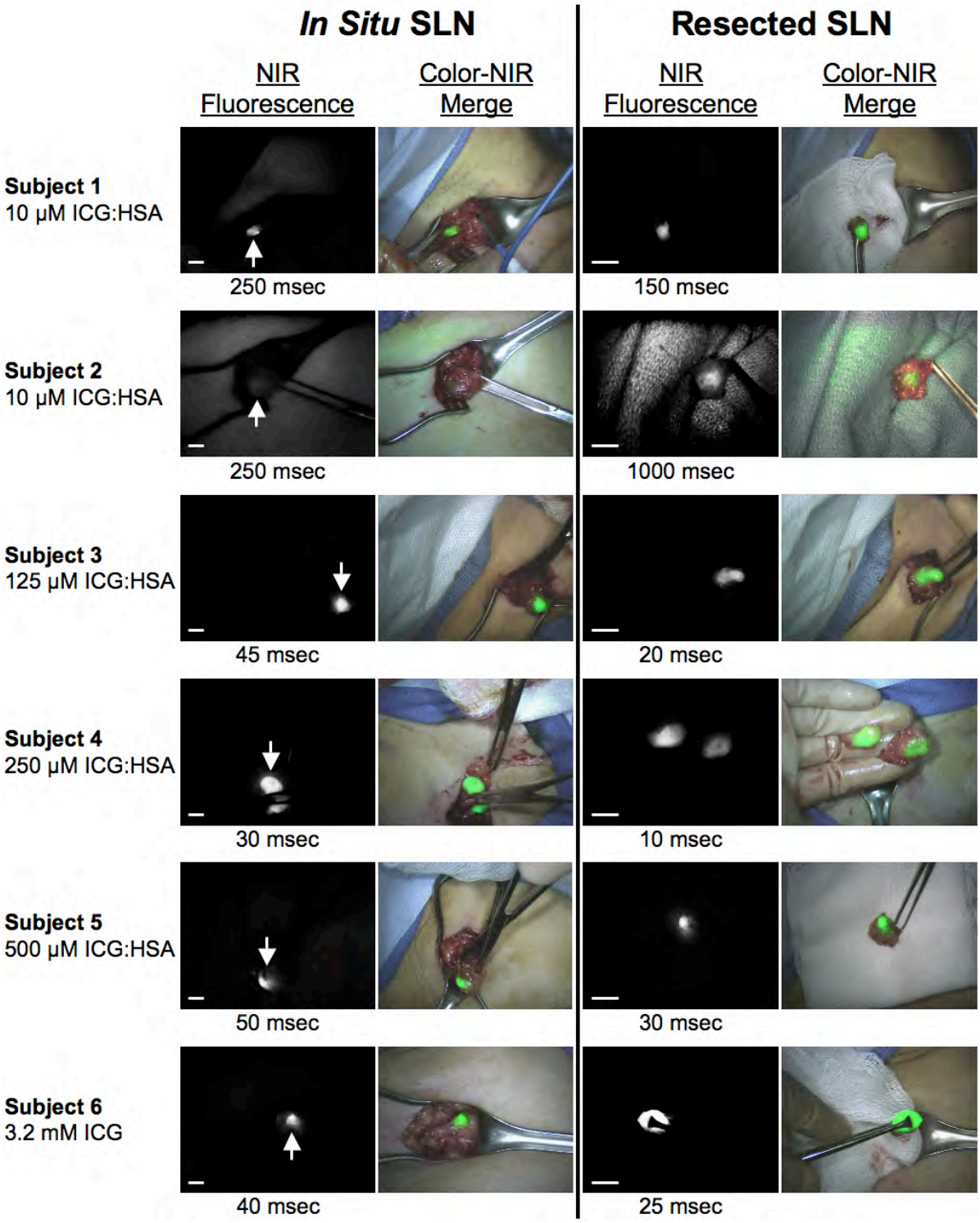

Supplementary Figure 4 - The Tradeoff between NIR Fluorophore Quenching and Lymphatic System Dilution during SLN Mapping in Women with Breast Cancer: The subject number, concentration of injected NIR fluorophore, and type of NIR fluorophore are noted on the left. *In situ* (left; arrows) and resected (right) SLNs are shown, with corresponding 800 nm NIR fluorescence images (left columns) and a merge of color video and NIR fluorescence (right). ICG fluorescence is pseudo-colored in lime green in the Color-NIR Merge images. 760-nm excitation fluence rate was ≈ 7.7 mW/cm^2 for all images. The camera exposure time employed is indicated below each NIR fluorescence image. Scale bars indicate 1 cm.

The first two patients in the series received 10-μM ICG:HSA, the same concentration used in our original FLARE™ study.[4] Although detectable, the final SBR in the SLN was relatively low and variable, it was not always possible to clearly visualize lymphatic channels traveling from the injection site to the SLNs, and camera exposure times were long. Increasing the concentration of ICG:HSA up to 500 μM resulted in visualization of lymphatic channels, progressively higher SBRs in the SLNs, and shorter camera exposure times, despite the fact that fluorescence at the injection site was severely quenched (data not shown).

The final subject received non-diluted (3.2 mM) ICG without pre-adsorption to HSA. In this case, although lymph nodes were identified with high SBR, background staining in the axilla was extremely high, and one of the resected nodes was negative by ^{99m}Tc-sulfur colloid lymphoscintigraphy, suggesting possible flow of ICG past the SLN into second tier nodes. Overall, a total of 12 lymph nodes were identified by ^{99m}Tc-sulfur colloid lymphoscintigraphy and 13 by NIR fluorescence.

SUPPLEMENTARY DISCUSSION

For oncologic surgery, one channel of FLARE™ or Mini-FLARE™ can be used to remove malignant cells, while the second can be used to avoid blood vessels or nerves. For sentinel lymph node (SLN) mapping, one channel can be used to identify SLN(s), while the other could be used to find all lymph nodes in the basin, for example, during a completion lymphadenectomy, or to avoid nearby blood vessels or nerves.

Much of the reduction in cost and weight of Mini-FLARE™ results from using only a single non-cooled NIR camera rather than two cooled NIR cameras; the two NIR channels are created by cycling the excitation light (Figure 1C) and employing a dual bandpass emission filter (Supplementary Figure 2). Although this strategy can effectively separate different 700-nm and 800-nm NIR fluorophores (Supplementary Figure 3), many NIR fluorophores have significant overlap in their absorption and emission spectra (Supplementary Figure 2), requiring careful consideration of fluence rates and concentrations before interpreting results. Although, use of a single 700-nm or 800-nm NIR fluorophore with Mini-FLARE™, appears to work well. Given the current trend in the field to miniaturize surgical imaging sytems,[5] it is likely that future versions of Mini-FLARE™ will be able to restore full performance with an even smaller size.

Clinical translation of new medical imaging devices, such as Mini-FLARE™, is difficult. Our group has recently published a detailed algorithm to facilitate such translation.[6] Using this strategy, we successfully performed a first-in-human clinical trial of Mini-FLARE™ during breast cancer sentinel lymph node mapping. Since no adverse events or alterations in providing the standard of care were noted with Mini-FLARE™, the study achieved its primary objective.

In our 24-patient clinical study, two patients experienced a wound infection requiring antibiotics and one patient underwent surgical re-exploration because of an expanding hematoma following axillary lymph node dissection, resulting in a complication rate of 12.5%. This rate is within the commonly reported range of complications following breast and axillary surgery.[7-9] ICG has been used in clinical practice since 1958. The only reported adverse reactions are anaphylactic, which are generally mild unless in the setting of renal failure and high dose administration. Therefore, it seems unlikely that the complications that occurred in the current study are the result of ICG administration. Time to detection of the SLN was relatively short in our study (average time between skin incision and SLN resection was 17 minutes ± 5). Although our study was not designed to compare detection time of NIR only with that of the combined use of Tc-99m and patent blue dye, it seems likely that the use of NIR fluorescence did speed up detection. Quicker detection of SLN has the advantage of less anesthesia time, higher patient turnover, and better hospital efficiency.

Previous clinical studies that tested NIR fluorescence SLN mapping used ICG alone instead of ICH:HSA,[10-14] except for Troyan et al.[4] Theoretically, the injection of ICG alone results in poor retention of the lymphatic tracer in the SLN, which as a consequence results in fluorescent staining of higher tier nodes and background staining of the axilla. Although not compared directly, studies using ICG alone reported a higher average number of identified SLNs (range = 1.8 – 5.4; aggregate average = 3.4),[10-14] than with the use of ICG:HSA (Troyan et al.[4]: 1.5; current study: 1.45). In the current study, no additional nodes were identified by NIR fluorescence that were neither radioactive nor blue, suggesting retention of ICG:HSA in the SLN. Although comparison of these data are difficult because the concentration of ICG alone used was significantly higher (typically 6.4 mM) than in the trials using ICG:HSA (10 μM to 1000 μM), this finding suggests that ICG:HSA may indeed provide better retention in the SLN. A study directly comparing ICG to ICG:HSA is ongoing.

SUPPLEMENTARY TABLES

Supplementary Table 1 – 6-Patient Pilot Study Subject Characteristics

Subject	Age (yr)	Height (ft)	Weigh t (lbs)	Body Mass Index	Skin Type	Location of Primary Tumor(s)	Size of Primary Tumor(s)	Histological Type	Histo-logical Grade
1	49	5'0"	140	27.3	III	Rt; UC	1.5 cm	ICDL/DCIS	II
2	64	5'3"	129	22.8	III	Rt; LI	1.3 cm	IDC	I
3	47	5'8"	271	41.2	I	Lt; UO	1.1 cm	ICDL/DCIS	II
4	69	5'7"	167	26.2	II/III	Rt; UO	0.9 cm	IDC/DCIS	II
5	71	5'1"	130	24.6	II	Lt; UI Lt; UO	0.7 cm 0.6 cm	ILC ILC	I I
6	61	5'1"	216	40.8	III	Rt; UC	2.3 cm	ICDL	II

Skin Type = American Academy of Dermatology Skin Types I-VI:

I. Pale white skin: Always burns easily; never tans (Celtic, Scandinavian, and infants)
II. White: Usually burns easily; tans minimally (Northern European)
III. White (average): Sometimes burns; tans gradually to light brown (Central European)
IV. Beige or lightly tanned: Burns minimally; always tans to moderately brown (Mediterranean, Asian)
V. Moderate brown or tanned: Rarely burns; tans well (South American, Indian, Native American)
VI. Dark brown or black: Never burns; deeply pigmented (African, African-American, Aborigine)

Location of Primary Tumor: Lt = Left; Rt = Right. C = Center; I = Inner; L = Lower; O = Outer; U = Upper.

Histological Types: IDC = Invasive ductal carcinoma; ILC = Intralobular carcinoma; ICDL = Invasive carcinoma with ductal and lobular features; DCIS = Ductal carcinoma *in situ*.

Histological Grades: I = Low-grade; II = Intermediate grade; III = High-grade.

Supplementary Table 2 – Identification of SLNs by Lymphoscintigraphy and NIR Fluorescence in the 6-Patient Pilot Study

Subject	NIR Lymphatic Tracer (Concentration)	Node #	Histology	Radioactive Detection	NIR Fluorescence Detection	
				Count Rate (cps)	SBR of *In Situ* SLN (Exp. Time)	SBR of *Ex Vivo* SLN (Exp. Time)
1	ICG:HSA (10 μM)	1	+	4670	7.3 (250 msec)	4.3 (150 msec)
		2	-	1712	1.1 (250 msec)	2.1 (250 msec)
		3	-	1356	1.7 (250 msec)	1.3 (500 msec)
2	ICG:HSA (10 μM)	1	+	318	2.1 (250 msec)	1.8 (1000 msec)
3	ICG:HSA (125 μM)	1	-	8296	15.0 (45 msec)	19.3(20 msec)
4	ICG:HSA (250 μM)	1	-	934	30.7 (30 msec)	26.1 (10 msec)
		2	-	2006	20.8 (30 msec)	13.3 (10 msec)
		3	-	427	3.4 (200 msec)	16.9 (40 msec)
5	ICG:HSA (500 μM)	1	-	1261	15.6 (50 msec)	34.5 (30 msec)
		2	-	397	7.9 (50 msec)	9.0 (60 msec)
6	ICG (3.2 mM)	1	-	2941	10.6 (40 msec)	25.1 (25 msec)
		2	-	<30	20.2 (20 msec)	5.5 (35 msec)
		3	-	397	4.4 (50 msec)	8.2 (50 msec)
			Total Lymph Nodes Detected	**12**	**13**	

ICG = Indocyanine green; ICG:HSA = Indocyanine green adsorbed to human serum albumin (HSA).

Histology: (-) = no evidence of metastasis; (m) = micrometastases < 1 mm; (+) = metastases ≥ 1 mm.

SBR = NIR fluorescence signal-to-background ratio of SLN (signal) to surrounding nodal tissue (background).

Exp. Time = NIR camera exposure time needed to achieve this SBR using an excitation fluence rate of 7.7 mW/cm^2.

SUPPLEMENTARY REFERENCES

1. Gioux S, Kianzad V, Ciocan R, Gupta S, Oketokoun R, Frangioni JV. High-power, computer-controlled, light-emitting diode-based light sources for fluorescence imaging and image-guided surgery. Mol Imaging 2009; 8:156-65.
2. Gioux S, De Grand AM, Lee DS, Yazdanfar S, Idoine JD, Lomnes SJ, Frangioni JV. Improved optical sub-systems for intraoperative near-infrared fluorescence imaging. SPIE Proceedings 2005; 6009:39-48.
3. Gioux S, Ashitate Y, Hutteman M, Frangioni JV. Motion-gated acquisition for in vivo optical imaging. J Biomed Opt 2009; 14:064038.
4. Troyan SL, Kianzad V, Gibbs-Strauss SL, et al. The FLARE intraoperative near-infrared fluorescence imaging system: a first-in-human clinical trial in breast cancer sentinel lymph node mapping. Ann Surg Oncol 2009; 16:2943-52.
5. Wang X, Bhaumik S, Li Q, Staudinger VP, Yazdanfar S. Compact instrument for fluorescence image-guided surgery. J Biomed Opt 2010; 15:020509.
6. Gibbs-Strauss SL, Rosenberg M, Clough BL, Troyan SL, Frangioni JV. First-in-human clinical trials of imaging devices: an example from optical imaging. Conf Proc IEEE Eng Med Biol Soc 2009; 2009:2001-4.
7. Langer I, Guller U, Berclaz G, et al. Morbidity of sentinel lymph node biopsy (SLN) alone versus SLN and completion axillary lymph node dissection after breast cancer surgery: a prospective Swiss multicenter study on 659 patients. Annals of Surgery 2007; 245:452-461.
8. Olson JA, Jr., McCall LM, Beitsch P, et al. Impact of immediate versus delayed axillary node dissection on surgical outcomes in breast cancer patients with positive sentinel nodes: results from American College of Surgeons Oncology Group Trials Z0010 and Z0011. Journal of Clinical Oncology 2008; 26:3530-3535.
9. Vitug AF, Newman LA. Complications in breast surgery. Surgical Clinics of North America 2007; 87:431-51, x.
10. Hirche C, Murawa D, Mohr Z, Kneif S, Hunerbein M. ICG fluorescence-guided sentinel node biopsy for axillary nodal staging in breast cancer. Breast Cancer Res Treat 2010; 121:373-8.
11. Hojo T, Nagao T, Kikuyama M, Akashi S, Kinoshita T. Evaluation of sentinel node biopsy by combined fluorescent and dye method and lymph flow for breast cancer. Breast 2010.
12. Kitai T, Inomoto T, Miwa M, Shikayama T. Fluorescence navigation with indocyanine green for detecting sentinel lymph nodes in breast cancer. Breast Cancer 2005; 12:211-215.

13. Murawa D, Hirche C, Dresel S, Hunerbein M. Sentinel lymph node biopsy in breast cancer guided by indocyanine green fluorescence. British Journal of Surgery 2009; 96:1289-1294.
14. Tagaya N, Yamazaki R, Nakagawa A, Abe A, Hamada K, Kubota K, Oyama T. Intraoperative identification of sentinel lymph nodes by near-infrared fluorescence imaging in patients with breast cancer. American Journal of Surgery 2008; 195:850-853.